JOURNAL OF
PESTICIDE SCIENCE

Regular Article

Degradation of the strobilurin fungicide mandestrobin in illuminated water–sediment systems

Takeshi Adachi,* Yusuke Suzuki and Takuo Fujisawa

Sumitomo Chemical Co., Ltd. Environmental Health Science Laboratory, 4–2–1 Takatsukasa, Takarazuka, Hyogo 665–8555, Japan

The degradation behavior of mandestrobin (**1**) was investigated in aerobic aquatic water–sediment systems exposed to continuous artificial sunlight ($\lambda > 290$ nm). [^{14}C]mandestrobin uniformly labeled at the phenoxy or benzyl ring was individually applied to the overlying water of the system at a rate equivalent to 262.5 g a.i./ha. The transformation of **1** was mainly proceeded *via* photoinduced bond cleavage at the benzyl phenyl ether and the subsequent rearrangement reaction. Interestingly, some of the photodegradates and microbial metabolites of **1** observed in the aquatic photodegradation and water–sediment (dark) studies, respectively, were never detected. Furthermore, the observed photoproducts were less formed and were steadily degraded or metabolized to carbon dioxide or strongly adsorbed to bottom sediment. The fate of **1** and its degradates in illuminated water–sediment systems was considered to reflect realistic conditions more precisely, as it accounts for various effects attributed to sunlight.
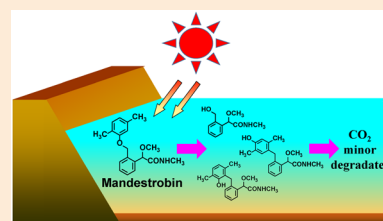
Keywords: mandestrobin, photodegradation, illuminated water–sediment system, natural water.

Introduction

Photodegradation is one of the important routes for transformation of pesticides in the natural environment.[1–3] Pesticides applied to agricultural fields show various degradation profiles by sunlight irradiation in natural water and on soil and plant surfaces.[4–7] In order to understand the fundamental behavior of pesticides in the aqueous environments, simulation studies of degradative processes such as hydrolysis, aqueous photolysis, and biodegradation in water–sediment systems in darkness are mandatory for registration of pesticides in the European Union (EU) in accordance with Organization for Economic Co-operation and Development (OECD) Guidelines 111, 316, and 308, respectively.[8–10] These standard studies are remarkably important to evaluate the environmental fate of pesticides under each defined test condition. However, it is difficult to elucidate the

* To whom correspondence should be addressed.
 E-mail: adachit7@sc.sumitomo-chem.co.jp
 Published online February 21, 2024

more realistic behavior of these chemicals in the natural aqueous environment from simply the results of these tests because multiple factors which are mutually and intricately involved in the fate of pesticides are not reflected in the systems used for testing. For example, the photosynthesis-driven pH elevation by algae and aquatic macrophytes occurs in sediment systems under illumination.[11] In addition, not only direct photolysis but also indirect photolysis induces the production of reactive oxygen species in the presence of natural components (*i.e.*, nitrate, nitrite, humic acid and chromophoric organic matter)[12–15] and *via* the absorption of natural sunlight. Furthermore, the resultant photo-unique products in overlying water sink to the bottom sediment where they undergo microbially mediated metabolism. These factors significantly contribute to the complicated degradation profile of pesticides.[16–19] Therefore, especially for the chemicals that have unique photo-degradation products, simulation studies performed under illuminated water–sediment system conditions together with the standard ones (OECD 111, 316 and 308) are necessary to accurately understand their behavior in the natural aqueous environment and potential risks to aquatic organisms.

Mandestrobin [(*RS*)-2-methoxy-*N*-methyl-2-[α-(2,5-xylyloxy)-*o*-tolyl]acetamide], **1**, is the strobilurin fungicide commercially developed by Sumitomo Chemical Co., Ltd. The aqueous simulation studies in buffered solution showed that **1** is resistant to

hydrolysis in the pH range of 4 to 9[20)] and is rapidly photodegraded with the half-life of 8.6–12.8 days (Tokyo, 35°N, spring) and 2.7–3.9 days (EU/US, 30–50°N).[12)] In the latter aqueous photolysis study, **1** is mainly photodegraded *via* homolytic cleavage of the benzyl phenyl ether bond to produce not only the corresponding alcohol derivative but also various unique degradation products such as intramolecular rearrangement isomers and a seven-membered heterocyclic compound, which are finally mineralized to carbon dioxide.[12)] No photoinduced isomerization at the 2-position of the acetamide moiety is observed.[12)] In the aerobic soil metabolism and water–sediment studies which are both conducted in darkness, **1** is more slowly metabolized or degraded *via* oxidation of either of the two methyl groups in the phenoxy ring to form monocarboxylic acid derivatives.[20)]

Incidentally, there is no published literature or information on the degradation profile of **1** under illuminated water–sediment system conditions, which are considered to reflect various important phenomena in nature. The objectives of this study were to clarify the degradation pathway of **1**, the possible accumulation of degradation products, and the non-generation of toxic degradates to aquatic organisms, using a modified water–sediment system under irradiation in comparison with systems of aqueous photolysis and water–sediment in darkness.

Materials and methods

1. Chemicals

Two radiolabels of **1**, uniformly labeled with ^{14}C at either phenyl ring, abbreviated as [BR-^{14}C]-**1** and [PX-^{14}C]-**1** (Fig. 1), were synthesized in our laboratory. The specific activities of [BR-^{14}C]-**1** and [PX-^{14}C]-**1** were 14.6 and 14.2 MBq/mg, respectively, and their radiochemical purities were determined to exceed 98%. Nonradiolabeled **1** and its related eight substances **2**–**9** were used as reference standards for the structural identification. Among them, **1**–**8** were prepared in our laboratory using previously reported methods.[12,21,22)] 2,5-Dimethylphenol **9** was purchased from Sigma-Aldrich Japan (Tokyo, Japan). Pure water was supplied from a Direct-Q 3UV water purification system ($>18\,M\Omega\,cm$, Merck Japan, Tokyo, Japan).

2. Spectroscopy and chromatography

The ultraviolet-visible (UV-vis) absorption spectra of **1** and surface water used in this study were measured using a UV-2550 UV-vis spectrometer (Shimadzu, Kyoto, Japan) with a quartz cuvette (1 cm path length).

An LC-20A series high performance liquid chromatography (HPLC) system (Shimadzu, Kyoto, Japan) equipped with a 150 mm×6.0 mm i.d., 5 μm, SUMIPAX ODS A-212 column (Sumika Chemical Analysis Service, Osaka, Japan) was operated at a flow rate of 1 mL/min using the following gradient program for analysis of the degradation profile: solvent A, 0.05% formic acid; solvent B, acetonitrile; 0 min, 5% B; 0–5 min, 5–100% B; concentration of B held at 100% until 60 min (Method 1). The retention times of reference standards were **1**/42.5 min, **2**/40.7 min, **3**/33.3 min, **4**/19.2 min, **5**/40.0 min, **6**/36.9 min,

7/34.1 min, **8**/31.8 min, and **9**/32.4 min. A CHIRALCEL AD-RH column (5 μm, 4.6-mm i.d.×150 mm, Daicel Chemical, Osaka, Japan) was used to determine the proportion of *R* and *S* isomers of **1** in the samples and elution was performed at a flow rate of 1 mL/min with acetonitrile/water＝1/1 (v/v) (Method 2). The typical retention times of *R* and *S* isomers were 15.8 min and 21.5 min, respectively. The radioactivity of column effluents was monitored with a Radiomatic 150TR detector equipped with a 500 μL liquid cell using Ultima-Flo AP liquid scintillation cocktail (PerkinElmer Japan, Kanagawa, Japan). Each ^{14}C peak was identified by HPLC co-chromatography by comparing its retention time with those of nonradiolabeled references detected at 254 nm with an SPD-20A UV detector (Shimadzu, Kyoto, Japan). To further confirm the chemical identity of each degradate detected by HPLC, two-dimensional thin-layer chromatography (2D-TLC) was conducted using silica gel 60F$_{254}$ thin-layer plates (200×200 mm, 0.25-mm layer thickness; Merck Japan, Tokyo, Japan) with the solvent systems of A (chloroform/methanol; 9:1, v/v) and B (*n*-hexane/2-propanol; 5:2, v/v). The R$_f$ values of reference standards were **1**/0.97, **2**/0.98, **3**/0.70, and **4**/0.73 for solvent system A and **1**/0.70, **2**/0.75, **3**/0.33, and **4**/0.61 for solvent system B. Radioactive regions on TLC plates were exposed to BAS III$_S$ imaging plates (Fuji Photo Film, Tokyo, Japan) and signal intensities were quantitated by a Typhoon 9200 Variable Mode Imager (GE Healthcare Japan, Tokyo, Japan). Nonradiolabeled references co-developed on TLC were visualized using UV light.

Liquid chromatography-mass spectrometry (LC-MS) in positive ion mode was performed by using a ZQ 2000 spectrometer (Waters Japan, Tokyo, Japan) with an ESCi multimode probe equipped with electrospray ionization (ESI) and atmospheric pressure chemical ionization (APCI) interface, which was connected to an Alliance HPLC system (Waters Japan, Tokyo, Japan). Samples were eluted using the same gradient system as Method 1 except for the flow rate 0.2 mL/min.

An ion chromatography system ICS-5000 (Thermo Fisher Scientific, Massachusetts, USA) was employed to determine the concentration of inorganic substances in the water samples. The operating parameters and equipment were as follows: a DIONEX Ion Pak AS23 (250 mm×4 mm i.d., Thermo Fisher Scientific, Massachusetts, USA) was used as analytical column with a DIONEX Ion Pak AG23 (50 mm×4 mm i.d., Thermo Fisher Scientific, Massachusetts, USA) as guard column; a solution containing 4.5 mmol/L Na_2CO_3 and 0.8 mmol/L $NaHCO_3$ was used as eluent at a flow rate of 1 mL/min; chemical suppression; sample loop volume of 10 μL. The typical retention times of chloride, nitrite, nitrate, and sulfate ions were 8.1 min, 10.2 min, 15.3 min, and 30.3 min, respectively.

3. Radioassay

The radioactivity in aliquots of photolysis test solutions, trapping media, and rinsates of glass surfaces was individually determined in duplicate by mixing each aliquot with 10 mL of Emulsifier Scintillator Plus (PerkinElmer Japan, Kanagawa, Japan)
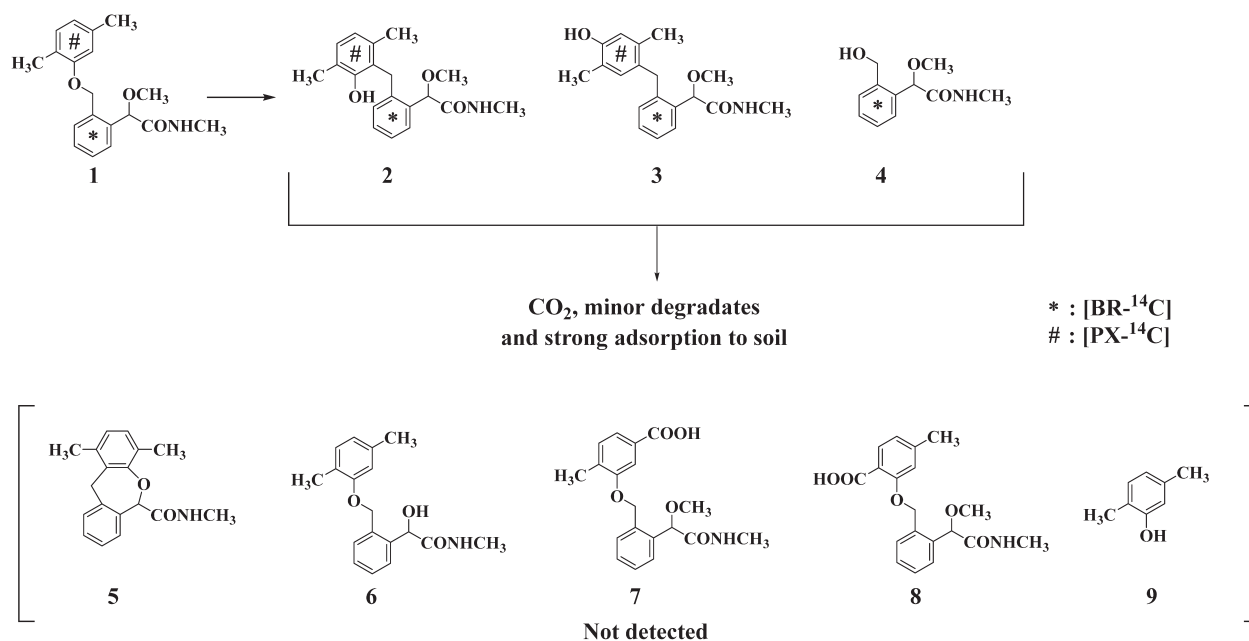
Fig. 1. Proposed photolysis pathways of **1** in an illuminated water–sediment system. ¹⁴C labeled positions of **1**: *, [BR-¹⁴C]-**1**; #, [PX-¹⁴C]-**1**.

and then analyzed by liquid scintillation counting (LSC) for 5 min with a Tri-Carb 3110 TR liquid scintillation spectrometer (PerkinElmer Japan, Kanagawa, Japan). The amounts of ^{14}C collected in 0.5 M NaOH traps were determined as $^{14}CO_2$ by adding 1.0 M $BaCl_2$, resulting in quantitative precipitation as $Ba^{14}CO_3$. The background level of all samples was 0.5 Bq.

4. Test system

A bottom sediment and overlying water were collected from Golden Lake (North Dakota, USA) and stored in a refrigerator at 4°C until use. The textural class of the used soil was sand with organic carbon 0.57%, and pH 8.0 in soil/water=1/1 (v/v) ratio. The test apparatus was prepared in accordance with the previous method.[19] A 50-g sediment sample was taken into a two-necked cylindrical glass vessel (4.4 cm i.d.) to a depth of 2 cm, and then the overlying water was added to each vessel to a depth of 6 cm. The applied solutions were prepared in acetonitrile with [BR-^{14}C]-**1** and [PX-^{14}C]-**1** at concentrations of approximately 259 kBq/mL and 191 kBq/mL, respectively. For each label, test system for the light irradiation and the dark control was prepared in singlicate. After a pre-incubation period of a month for water–sediment samples, 140 μL and 178 μL of the above solutions of [BR-^{14}C]-**1** and [PX-^{14}C]-**1**, respectively, were applied to the water surface in each vessel at a rate of 2.4 μg/vessel using a microsyringe, which is equivalent to the field application rate of 262.5 g a.i./ha assuming its uniform distribution in the water layer to a depth of 100 cm. The glass vessel including each water–sediment system was immersed in a water bath maintained at 20±2°C and set on an orbital shaker (MK-200D, Yamato Scientific, Tokyo, Japan) at 20 rpm to moderately mix the water phase without disturbance of the sediment. Humidified air was successively passed over the water surface to ethylene glycol

and alkaline traps in sequence for collection of organic volatiles and carbon dioxide, respectively, in the same manner as previously reported.[19] Each vessel was continuously irradiated using an Atlas Suntest XLS+ 2-kW xenon arc lamp (Toyo Seiki, Tokyo, Japan) through the Pyrex inner filter to remove UV light at wavelengths below 290 nm. The light intensity was almost constant throughout the study with its irradiance at 300–400 nm as 36.5 and 46.4 W/m² for [BR-^{14}C]-**1** and [PX-^{14}C]-**1** labeled studies, respectively. Since the light intensity of Xe lamp was different in each study, it was converted to the typical natural sunlight intensity according to the J-MAFF (Tokyo, 35°N, spring)[23] and OECD test guidelines (EU/US, 30–50°N, summer).[24] The same system, established as the dark control, was maintained at 20± 2°C in a SR-30VE2 incubator (Nagano Science, Osaka, Japan) without illumination. The overlying water and associated sediment were separately analyzed at 0, 4, 7, 14, and 28 days after application. At each sampling, the pH and oxidation-reduction potential (ORP) values of the water and sediment layers were individually monitored by an F-22 pH-meter equipped with pH and ORP electrodes (Horiba, Kyoto, Japan). In addition, the dissolved oxygen content (DO) in the water layer was measured with a DO-8F DO-meter (Horiba, Kyoto, Japan).

The overlying water was collected by decantation, directly radioassayed by LSC, and then extracted twice with ethyl acetate. A portion of the combined extract (ethyl acetate layers) was concentrated *in vacuo* for HPLC analysis. The sediment was transferred to a centrifugal bottle and extracted by shaking with acetone/0.1 M HCl (5:1, v/v) in a mechanical shaker for 10 min. After shaking, the bottle was centrifuged for 10 min at 10,000 rpm, and the supernatant was collected by decantation. The extraction was repeated three times in the same manner. All the collected supernatants were put into a single flask. Then, an

aliquot was evaporated to remove acetone which was extracted twice with ethyl acetate. A portion of the combined ethyl acetate layers was individually radioassayed by LSC and was concentrated *in vacuo* for HPLC analysis. The chemical identity of each radiolabeled compound was confirmed by comparing its HPLC retention time and its TLC R$_f$ value with those of the nonradiolabeled reference standards. The unextractable sediment residue (bound residue ^{14}C) was air-dried and combusted for radioassay. The selected unextractable residue was further fractionated by the Soxhlet method with acetone/0.1 M HCl (5 : 1, v/v) 15 times for characterization of the radioactivity.

Apart from the above exhaustive extraction, the 28-day soil samples of both labels were individually extracted by the following silylation method in order to release the objective chemicals from sediment by breaking hydrogen bond interactions between ^{14}C-labeled compounds and the sediment constituents.[25] A 2.0-g sample of dried matrix material was taken and mixed with 120 mL of chloroform, 6.0 g of NaOH, and 20 mL of trimethylchlorosilane, and then the mixture was stirred at room temperature under argon during the reaction. After 3 hr of stirring, 6.0 g of NaOH and 20 mL trimethylchlorosilane were re-added for overnight reaction. Finally, the chloroform layer was removed by decantation from the reaction mixture and the soil residue was extracted with 40 mL acetone three times. These chloroform and acetone extracts were combined and centrifuged, and the radioactivities therein were measured by LSC.

Degradation curves of **1** were fitted to a single first-order (SFO) model according to Forum for the coordination of pesticide fate models and their use (FOCUS) recommendations[26] and half-life values were estimated by using Computer Assisted Kinetic Evaluation (CAKE v. 3.1, Tessella, Oxford, United Kingdom) software.

Results

1. Spectroscopy and ion chromatography analyses

The UV-vis absorption spectra were measured for pure water with 10% acetonitrile dissolving **1** at a concentration of 0.1 mM and the overlying surface water used in this illuminated water–sediment study. The UV-vis absorption spectrum of **1** was shown as 500 times the intensity of the test concentration in Fig. 2. The absorption shoulders of **1** at wavelengths exceeding
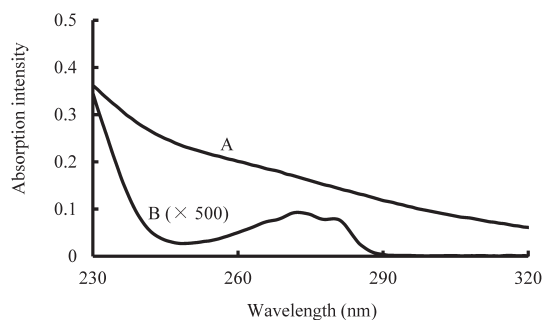

Fig. 2. Absorption spectra of natural water used in this study (A) and **1** in water containing 10% acetonitrile (B: ×500).

290 nm were slightly observed, and overlapped with the emission spectrum of xenon arc lamp light transmitted through the cut filter ($\lambda > 290$ nm), indicating that the direct photodegradation of **1** possibly proceeds in sunlit surface water.

The concentrations of inorganic ions in the test solutions before and after irradiation were measured by ion chromatography. The nitrate and nitrite ions which could serve as photosensitizers[13] were not observed throughout the study, whereas chloride and sulfate ions were detected at the concentration of 39 and 1167 mg/L before irradiation and 41 and 1654 mg/L after irradiation, respectively.

*2. Photodegradation study of **1***

2.1. Condition of the water–sediment system

The measured pH, ORP, and DO values in the overlying water and sediment throughout the studies are listed in Tables 1 and 2. The pH and DO values for each label did not significantly change during the study period. The ORP values were approximately 150–300 mV in the water phase and below 0 mV in the sediment.

2.2. Distribution of the radioactivity

The ^{14}C distribution within the test system individually treated with [BR-^{14}C]-**1** and [PX-^{14}C]-**1** under irradiated conditions and [BR-^{14}C]-**1** under dark conditions are summarized in Tables 1 and 2. Good ^{14}C recovery in the range 90.1–107.6% of the applied radioactivity (AR) was obtained throughout the study. The ^{14}C adsorbed onto the inner vessel wall was <1.0% AR, therefore, the adsorption of **1** and its degradation products to the apparatus was negligible. Upon exposure to light, most of **1** degraded or completely disappeared from the aqueous layer while gradually and steadily degraded to 12.6–18.5% AR in the sediment at the end of the study (28 days). The half-lives of **1** were estimated to be 4.4–6.1 days in the aqueous layer and 8.2–11 days in the total test system where the latter is equivalent to 49–50 days (Tokyo, 35°N, spring)[23] and 15 days (EU/US, 30–50°N, summer)[24] under natural sunlight (Table 3), indicating that the degradation rates were almost the same between [BR-^{14}C] and [PX-^{14}C] labels. In contrast, in darkness, the remaining amount of unchanged **1** was >90% AR with insignificant appearance of any degradation products exceeding 0.6% AR. In addition, the accumulated amount of volatile and adsorbed ^{14}C was 1.4% and less than 5% AR, respectively, and therefore, **1** was assumed to be comparatively stable in darkness throughout the study.

2.3. Identification and quantification of the degrades

The chemical structures of all major degrades were successfully confirmed by HPLC and TLC co-chromatography with the corresponding reference standards. The profile of degradation products under irradiated and dark conditions is summarized in Tables 1 and 2. The chiral HPLC analysis (Method 2) of **1** showed no photoinduced isomerization occurred at the 2-position of the acetamide moiety (data not shown). The photo rearrangement product **2** was primarily observed in the aqueous layer, maximally increased up to 5.9–11.2% AR after 4 days,

Table 1.   Distribution of [BR-^{14}C]-**1** in an illuminated water–sediment system and dark control

		% of the applied ^{14}C								
		Light irradiation					Dark control			
	Days	0	4	7	14	28	4	7	14	28
Volatile ^{14}C		na	0.5	1.5	4.9	11.3	0.2	0.3	0.8	1.4
	^{14}CO$_2$	na	0.5	1.5	4.9	11.2	0.2	0.3	0.8	1.4
	Others	na	nd	nd	nd	0.1	nd	nd	nd	nd
Aqueous ^{14}C		99.5	74.7	60.4	60.2	55.1	72.7	59.6	57.4	36.0
	1	99.1	57.9	48.2	21.0	nd	72.5	59.6	57.1	35.7
	2	nd	11.2	1.1	nd	nd	nd	nd	nd	nd
	3	nd	1.2	1.8	nd	nd	nd	nd	nd	nd
	4	nd	0.8	6.3	4.2	2.1	nd	nd	nd	nd
	5–8	nd	nd	nd	nd	nd	nd	nd	nd	nd
	Others	0.4	3.6	3.1	35.0	53.0	0.2	nd	0.3	0.3
Sediment ^{14}C		0.9	25.1	22.9	21.7	14.4	24.6	36.8	41.7	55.4
	1	0.8	22.4	20.0	19.5	12.6	24.6	36.8	41.2	54.8
	2	nd	nd	0.8	nd	nd	nd	nd	nd	nd
	3	nd	nd	0.3	nd	nd	nd	nd	nd	nd
	4	nd	nd	0.4	0.2	0.1	nd	nd	nd	nd
	5–8	nd	nd	nd	nd	nd	nd	nd	nd	nd
	Others	0.1	2.7	1.4	2.0	1.7	nd	nd	0.5	0.6
Total 1		99.9	80.3	68.2	40.5	12.6	97.1	96.4	98.3	90.5
Bound residue ^{14}C		nd	2.5	8.7	9.9	16.8	2.0	4.8	4.8	4.9
Total ^{14}C		100.4	102.8	93.5	96.7	97.6	99.5	101.5	104.8	97.7
	Aqueous ORP (mV)	312	248	213	236	229	259	151	201	263
	pH	7.89	8.61	8.54	8.69	8.67	8.41	8.46	8.51	8.65
	DO (ppm)	4.7	3.9	3.8	3.7	4.1	4.0	3.4	3.1	5.2
	Sediment ORP (mV)	−82	−60	−11	−62	20	−58	−59	−62	2
	pH	7.41	8.12	8.16	8.34	8.19	8.28	7.60	8.28	8.06

na: Not analyzed. nd: not detected.
Others: Consist of multiple components, none of which exceed 5.7% AR.

and quickly disappeared from the total system. Other minor products **3** and **4** amounted to 2.1–3.5% AR after 4–7 days and 6.7% AR after 7 days in the total system, respectively, and rapidly degraded thereafter. Interestingly, although **4** was formed *via* cleavage of the benzyl phenyl ether bond at maximum 6.7% AR in the total system, the corresponding counter structure, phenol derivative **9**, has never been detected for [PX-^{14}C] label throughout the study. In addition, other potential degradation products **5–8**, formed in the aqueous photolysis or aerobic soil metabolism study,[20] were not detected in the present illuminated water–sediment systems. There were numerous unidentified peaks which did not co-elute with any of the reference substances, but none of them amounted to >6.5% AR with no detection of the same component exceeding 5% AR at two sequential sampling points or with no increasing trend at the last sampling times, which is the EU's definition of a relevant metabolite in the environment.[27] Sum of volatile ^{14}C observed in the alkaline and ethylene glycol traps amounted to 11.3% AR for [BR-^{14}C] and 30.8% AR for [PX-^{14}C] label at the end of the study, where most

of the radioactivity therein was confirmed to be ^{14}CO$_2$.

For irradiated samples, the combustion analysis showed that the amount of bound residue ^{14}C in the sediment after acid extraction at room temperature (Tables 1 and 2) was 16.8–23.3% AR at the end of the study. Successive exhaustive harsh extraction using the same acid solvent with high temperature released only a trace amount of ^{14}C from the sediment (3.0–4.4% AR). In addition, bound residue ^{14}C was characterized using a different method, *i.e.*, silylation, and as a result, an insignificant amount of the radioactivity was detected in the extracted solution (<2.4% AR).

Discussion

The degradation rate of **1** in the total illuminated water–sediment system (half-life of 49–50 days, Tokyo, 35°N, spring) was remarkably faster than that of the standard system in darkness (half-life of 248 days), indicating that the light irradiation significantly contributed to the decomposition of **1** (Fig. 3). Whereas its degradation in the illuminated water–sediment system was

**Table 2.** Distribution of [PX-^{14}C]-**1** in an illuminated water–sediment system

		% of the applied ^{14}C				
Days		0	4	7	14	28
Volatile ^{14}C		na	1.9	7.7	16.9	30.8
	^{14}CO$_2$	na	1.6	7.5	16.8	29.2
	Others	na	0.3	0.2	0.1	1.6
Aqueous ^{14}C		94.8	73.6	53.2	35.0	14.8
	1	93.5	47.9	38.3	3.2	2.5
	2	nd	5.9	4.5	nd	nd
	3	nd	3.5	2.2	nd	nd
	5–9	nd	nd	nd	nd	nd
	Others	1.3	16.2	8.3	31.8	12.3
Sediment ^{14}C		4.1	26.6	19.7	27.8	21.2
	1	4.0	22.9	14.5	19.2	18.5
	2	nd	nd	0.5	nd	nd
	3	nd	nd	0.5	nd	nd
	5–9	nd	nd	nd	nd	nd
	Others	0.1	3.7	4.2	8.4	2.7
Total 1		97.5	70.8	52.8	22.4	21.0
Bound residue ^{14}C		0.2	5.5	10.0	15.8	23.3
Total ^{14}C		99.1	107.6	90.6	95.5	90.1
Aqueous ORP (mV)		210	195	151	163	172
pH		8.59	8.52	8.52	8.41	8.61
DO (ppm)		5.7	4.1	4.2	3.9	6.9
Sediment ORP (mV)		−80	−51	−180	−172	−85
pH		8.07	7.86	8.16	8.09	8.30

na: Not analyzed.

nd: Not detected. Others: Consist of multiple components, none of which exceed 6.5% AR.

clearly restricted compared to the photolytic reaction in the homogeneous aqueous solution (half-life of 8–13 days, Tokyo, 35°N, spring).[12] For the latter phenomenon, one possible reason for the difference in degradation rate of **1** was the presence of dissolved organic matter in water. Concretely, the absorption light intensity of overlying surface water at 290 nm (1.2×10^{-1}) was remarkably greater than that of **1** (7.6×10^{-6}) as shown Fig. 2, and the same trend was also confirmed for wavelengths >290 nm. This finding implies that the direct photodegradation of **1** was suppressed by light shielding in the presence of dissolved organic matter in surface water.

Based on the results of ORP, DO, and pH, the water phase was demonstrated as aerobic condition and the sediment phase as anaerobic one. In such anaerobic conditions (*i.e.*, sediment), since biodegradation of **1** by aerobic bacteria does not occur, the presence of inorganic substances in natural water is generally considered to contribute to the acceleration of degradation. However, the nitrate[13,28,29] and nitrite[30,31] ions, which are known to be involved in the indirect photochemical process as photosensitizers, were not detected in the overlying water by
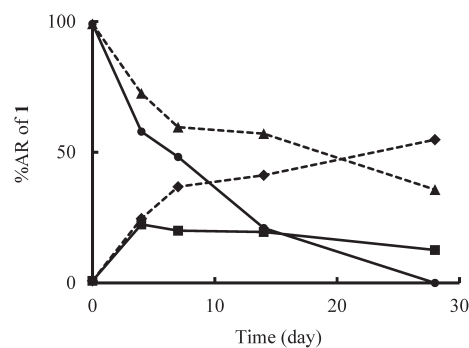
Fig. 3. Degradation behavior of [BR-^{14}C]-**1** in the irradiated system (solid line, ●: water phase and ■: sediment) and dark control system (dashed line, ▲: water phase and ◆: sediment).

ion chromatography analysis. Instead, chloride and sulfate ions were detected in the utilized water, but these inorganic ions and salts have no light absorption bands over 290 nm.[32] In fact, neither the chlorinated nor sulfidated form of **1** or its degradates were observed throughout the study by LC-MS analysis (data not shown). Therefore, the contribution of these inorganic substances to the photodegradation of **1** was considered to be minor throughout the study.

The decline curve analysis of **1** was conducted by assuming a single first-order kinetics in surface water with CAKE.[26] The behavior of **1** in overlying water can be explained by moderate partition to the bottom sediment (*i.e.*, dissipation), as indicated by the soil partition coefficient (K_{Foc}) value of 449,[20] and the photochemical reaction in the surface water (*i.e.*, degradation). Since **1** was stable in darkness, its decline rate in overlying water ($k=0.039$) was considered to correspond specifically with its rate of partition (dissipation) to bottom sediment. Then, the degradation rate constant related to only photolysis was conveniently estimated as $k=0.071-0.12$ by subtracting the rate constant under the dark condition ($k=0.039$) from that of illuminated systems ($k=0.11-0.16$). This calculation also demonstrated that the photolytic reaction in overlaying water of the water–sediment system was retarded as compared with the homogeneous aqueous solution ($k=0.22-0.32$) (Table 4).

As shown in Fig. 1, the primary photodegradation process of

Table 3. Half-lives of **1** in an illuminated and dark water–sediment system

Test condition		Xe lamp (day)	J-MAFF[23] (day)	OECD[24] (day)
[BR-^{14}C] light	Aqueous	6.1	—	—
	Total	11	50	15
[PX-^{14}C] light	Aqueous	4.4	—	—
	Total	8.2	49	15
[BR-^{14}C] Dark	Aqueous	18	—	—
	Total	248	—	—

J-MAFF, Ministry of Agriculture, Fisheries and Forestry of Japan.
OECD, Organization for Economic Co-operation and Development.

Table 4.   Kinetics analysis of dissipation of **1** under light irradiation and dark conditions based on the calculation by CAKE

System	Rate constant k (per day)	
	[BR-^{14}C]	[PX-^{14}C]
Decline rate in surface water with irradiation	0.11	0.16
Decline rate in surface water under dark conditions	0.039	—
Contribution of irradiation to the decline rate in surface water	0.071	0.12
Decline rate in homogeneous aqueous solution with irradiation[12]	0.32	0.22

1 can be initiated *via* homolytic cleavage of the benzyl phenyl ether bond followed by subsequent recoupling of the resultant radicals to form **2** and **3** in irradiated shallow surface water. This well-known photo-Claisen rearrangement[33] was observed in the homogeneous aqueous photolysis of **1** in buffered solution.[12] After cleavage of the benzyl phenyl ether bond, the benzyl alcohol derivative **4** was produced by reaction of the corresponding benzyl radical with dissolved hydroxyl radical and hydroxide ion through indirect and direct photolysis, respectively.[12] On the other hand, the formation of rearrangement products induced by direct photolysis was accelerated by the in-cage reaction before the hydroxyl radical attacks to generate **4**.[12] In the case of **1**, the predominant formation of the rearrangement products **2** and **3** as compared to **4** suggested that the direct photoreaction mainly contributed to the degradation of **1** even in the illuminated water–sediment system. The unique seven-membered heterocyclic compound **5**, which is formed *via* cyclization of **2** in the homogeneous aqueous solutions,[12] has never been detected in the present water–sediment system, probably not only due to its successive degradation in the surface water by light but also its partition to the sediment followed by degradation before **5** could be generated. Likewise, the elimination or oxidation of the methyl group to form **6**–**8** did not proceed throughout the study. These microbially-derived metabolites (**6**–**8**) were only detected at less than 5.0% AR after 101 days in the water–sediment system in darkness,[34] which suggested that they were not the products of the major degradation route of **1** or were rapidly dissipated/degraded under illuminated water–sediment system conditions. Incidentally, the phenol derivative **9** has never been detected, but the amount of volatile ^{14}C evolved from the phenoxy label (28 days, 30.8% AR) was approximately three times higher than that from the benzyl label (28 days, 11.3% AR). This suggested that ring cleavage and subsequent degradation of the phenoxy ring proceeded more rapidly as compared with the benzyl moiety. A possible reason for this rapid degradation is the involvement of photogenerated phenoxy radicals, which quickly self-decomposed due to the shorter lifetime of the phenoxy radical ($\tau=1.25$ msec) than the benzyl radical ($\tau=30$ msec)[35] as discussed in the previous report.[12] Overall, the benzyl ring moiety was considered to generate numerous minor degradates (28 days, 53.0% AR) in surface water, whereas the phenoxy ring

was rapidly degraded and mineralized under illuminated conditions. The observed major products in this irradiated water–sediment systems are those detected in individual soil and aqueous photolysis studies[16–19] as similar to other pesticides, which were less toxic than **1** for aquatic organisms.[20]

In the total system in darkness, unchanged **1** existed as >90% AR and bound residue ^{14}C was less than 5% AR suggesting less biodegradation (Table 1). In contrast, a significant increase of bound residue ^{14}C was observed under light irradiation for both labels (16.8–23.3% AR). The increased formation of bound residue under light irradiation compared to the dark has also been confirmed in the illuminated water–sediment study of esfenvalerate, which undergoes a radical cleavage reaction as similar to **1**.[18] However, only trace amounts of the radioactivity were extracted from it by exhaustive acidic extraction or silylation alone. Especially, the latter method is considered to specifically break hydrogen bonding between the radioactive components and sediment constituents. These results clearly indicate that the radioactive photodegraded components of bound residue ^{14}C are strongly combined to the sediment *via* covalent bonding, and thus can be considered to have less environmental concern.[36]

In conclusion, **1** underwent cleavage of the benzyl phenyl ether bond to produce photo-rearrangement products as the direct photodegradation in surface water in the illuminated water–sediment study. However, any specific degradates formed *via* photoinduced cyclization or microbially mediated oxidation of the methyl group described in OECD 316 and 308, respectively, were not observed. In addition, we have shown that no major degradates more toxic than **1** to aquatic organisms were observed in this test systems. The radioactivity in the sediment was produced due to extremely strong covalent bonding between radioactive substances and bottom sediment constituents, which is unlikely to be simply released into the aquatic environment. These results obtained in this illuminated water–sediment systems were considered to reflect realistic conditions more precisely as compared to the respective systems, *i.e.*, aqueous photolysis and water–sediment in darkness.

References

1) T. Katagi: Direct photolysis mechanism of pesticides in water. *J. Pestic. Sci.* **43**, 57–72 (2018).
2) T. Katagi: Theoretical and organic chemical approaches to environmental behavior and metabolism of pesticides. *J. Pestic. Sci.* **45**, 166–176 (2020).
3) Y. Suzuki and T. Katagi: Novel fluorescence detection of free radicals generated in photolysis of fenvalerate. *J. Agric. Food Chem.* **56**, 10811–10816 (2008).
4) S. Halladja, A. Amine-Khodja, A. ter Halle, A. Boulkamh and C. Richard: Photolysis of fluometuron in the presence of natural water constituents. *Chemosphere* **69**, 1647–1654 (2007).
5) H. Nishimura, Y. Suzuki, M. Nishiyama, T. Fujisawa and T. Katagi: Photodegradation of insecticide metofluthrin on soil, clay minerals and glass surfaces. *J. Pestic. Sci.* **36**, 376–384 (2011).
6) Y. Suzuki, A. Lopez, M. Ponte, T. Fujisawa, L. O. Ruzo and T. Katagi:

Photoinduced oxidation of the insecticide phenothrin on soil surfaces. *J. Agric. Food Chem.* **59**, 10182–10190 (2011).

7) K. Matsushima, D. Ando, Y. Suzuki and T. Fujisawa: Metabolism of the pyrethroid insecticide momfluorothrin in lettuce (*Lactuca sativa* L.). *J. Agric. Food Chem.* **69**, 6156–6165 (2021).

8) OECD: Test No. 111: Hydrolysis as a Function of pH. *OECD Guidelines for Testing of Chemicals*; OECD Publishing: Paris, 2004. https://www.oecd-ilibrary.org/docserver/9789264069701-en.pdf?expires=1635464819&id=id&accname=guest&checksum=0AAE6637FF103698D1DD3A069192CD85 (accessed 23 January, 2024).

9) OECD: Test No. 316: Phototransformation of Chemicals in Waters-Direct Photolysis. *OECD Guidelines for Testing of Chemicals*; OECD Publishing: Paris, 2008; https://www.oecd-ilibrary.org/docserver/9789264067585-en.pdf?expires=1635465280&id=id&accname=guest&checksum=D4D4376BEDDB00532840903D9D2F39FF (accessed 23 January, 2024).

10) OECD: Test No. 308: Aerobic and Anaerobic Transformation in Aquatic Sediment Systems. *OECD Guidelines for Testing of Chemicals*; OECD Publishing: Paris, 2002; https://www.oecd-ilibrary.org/docserver/9789264070523-en.pdf?expires=1635470536&id=id&accname=guest&checksum=8C4F24EF89344CF970EF062F5D29658D (accessed 23 January, 2024).

11) T. Katagi: Pesticide behavior in modified water–sediment systems. *J. Pestic. Sci.* **41**, 121–132 (2016).

12) T. Adachi, Y. Suzuki, M. Nishiyama, R. Kodaka, T. Fujisawa and T. Katagi: Photodegradation of strobilurin fungicide mandestrobin in water. *J. Agric. Food Chem.* **66**, 8514–8521 (2018).

13) T. Adachi, Y. Suzuki and T. Fujisawa: Photodegradation of an anilide fungicide inpyrfluxam in water and nitrate aqueous solution. *J. Agric. Food Chem.* **69**, 12966–12973 (2021).

14) C. K. Remucal: The role of indirect photochemical degradation in the environmental fate of pesticides. *Environ. Sci. Process. Impacts* **16**, 628–653 (2014).

15) D. F. Wallace, L. H. Hand and R. G. Oliver: The role of indirect photolysis in limiting the persistence of crop protection products in surface waters. *Environ. Toxicol. Chem.* **29**, 575–581 (2010).

16) A. Shibata, R. Kodaka, T. Fujisawa and T. Katagi: Degradation of flumioxazin in illuminated water–sediment systems. *J. Agric. Food Chem.* **59**, 11186–11195 (2011).

17) R. Kodaka, S. E. Swales, C. Lewis and T. Katagi: Effect of illumination on degradation of pyriproxyfen in water–sediment system. *J. Pestic. Sci.* **36**, 33–40 (2011).

18) R. Kodaka, T. Sugano and T. Katagi: Degradation of esfenvalerate in illuminated water–sediment system. *J. Pestic. Sci.* **34**, 27–36 (2009).

19) R. Kodaka, T. Sugano and T. Katagi: Metabolism of uniconazole-P in water–sediment systems under illumination. *Environ. Toxicol. Chem.* **25**, 310–316 (2006).

20) EFSA: Conclusion on the peer review of the pesticide risk assessment of the active substance Mandestrobin. *EFSA J.* **13**, 1–72 (2015).

21) D. Ando, T. Fujisawa and T. Katagi: Metabolism of the strobilurin fungicide mandestrobin in wheat. *J. Agric. Food Chem.* **66**, 10154–10162 (2018).

22) S. Murata, M. Kurosawa and T. Fujisawa: Efficient synthesis of carbon-14 labeled metabolites of the strobilurin fungicide mandestrobin using biomimetic iron-porphyrin catalyzed oxidation. *J. Labelled Comp. Radiopharm.* **66**, 290–297 (2023).

23) JMAFF: Studies of photolytic fate in water (2-6-2). *Data Requirements for Supporting Registration of Pesticides No. 13-Seisan-3986*; JMAFF, 2001. https://www.env.go.jp/council/10dojo/y100-16/mat_05-2.pdf (accessed 23 January, 2024).

24) OECD: Proposal for a New Guideline, Phototransformation of Chemicals on Soil Surfaces. *OECD Guidelines for Testing of Chemicals*; OECD Publishing: Paris, 2002; http://www.oecd.org/chemical-safety/testing/2741541.pdf (accessed 23 January, 2024).

25) K. Okuda, D. Ando, Y. Suzuki and T. Fujisawa: Improved assessment of soil nonextractable residues of the pyrethroid insecticide cyphenothrin. *J. Agric. Food Chem.* **71**, 9687–9695 (2023).

26) FOCUS: Guidance Document on Estimating Persistence and Degradation Kinetics from Environmental Fate Studies on Pesticides in EU Registration. *Report of the FOCUS Work Group on Degradation Kinetics EC Document Reference Sanco/10058/2005 version 2.0*; FOCUS, 2006. https://esdac.jrc.ec.europa.eu/public_path/projects_data/focus/dk/docs/finalreportFOCDegKinetics.pdf (accessed 23 January, 2024).

27) EUROPEAN COMMISSION. Guidance document on the assessment of the relevance of metabolites in groundwater of substances regulated under Council Directive 91/414/EEC *Sanco/221/2000*; 2003; Assessment of the relevance of metabolites in groundwater, directive 91/414EEC (europa.eu) (accessed 23 January, 2024).

28) J. Mack and J. R. Bolton: Photochemistry of nitrate and nitrite in aqueous solution: a review. *J. Photochem. Photobiol. Chem.* **128**, 1–13 (1999).

29) A. Torrents, B. G. Anderson, S. Bilboulian, W. E. Johnson and C. J. Hapeman: Atrazine photolysis: Mechanistic investigations of direct and nitrate-mediated hydroxyl radical processes and the influence of dissolved organic carbon from the Chesapeake Bay. *Environ. Sci. Technol.* **31**, 1476–1482 (1997).

30) C. Lu, X. Yin, X. Liu and M. Wang: Study of the photodegradation kinetics and pathways of hexaflumuron in liquid media. *J. Photochem. Photobiol.* **90**, 1219–1223 (2014).

31) H. Boucheloukh, T. Sehili, N. Kouachi and K. Djebbar: Kinetic and analytical study of the photo-induced degradation of monuron by nitrates and nitrites under irradiation or in the dark. *Photochem. Photobiol. Sci.* **11**, 1339–1345 (2012).

32) R. P. Buck, S. Singhadeja and L. B. Rogers: Ultraviolet absorption spectra of some inorganic ions in aqueous solutions. *Anal. Chem.* **26**, 1240–1242 (1954).

33) F. Galindo: The photochemical rearrangement of aromatic ethers. A review of the photo-Claisen reaction. *J. Photochem. Photobiol. Chem.* **6**, 123–138 (2005).

34) R. Graham: Mandestrobin: Degradation in water–sediment systems under aerobic conditions. *Covance laboratories Ltd.* Unpublished work, (2011).

35) H. J. Timpe and H. J. Friedrich: Flash light spectroscopic study of photo-Claisen rearrangement of phenyl benzyl ether. *Z. Chem.* **16**, 369–370 (1976).

36) M. Kästner, K. M. Nowak, A. Miltner, S. Trapp and A. Schäffer: Classification and modelling of nonextractable residue (NER) formation of xenobiotics in soil – A Synthesis. *Crit. Rev. Environ. Sci. Technol.* **44**, 2107–2171 (2014).